
Piecewise Normalizing Flows

Harry Thomas Jones Bevins^{1,2} Will Handley^{1,2} Thomas Gessey-Jones^{1,2}

Abstract

Normalizing flows are an established approach for modelling complex probability densities through invertible transformations from a base distribution. However, the accuracy with which the target distribution can be captured by the normalizing flow is strongly influenced by the topology of the base distribution. A mismatch between the topology of the target and the base can result in a poor performance, as is typically the case for multi-modal problems. A number of different works have attempted to modify the topology of the base distribution to better match the target, either through the use of Gaussian Mixture Models (Izmailov et al., 2020; Ardizzone et al., 2020; Hagemann & Neumayer, 2021) or learned accept/reject sampling (Stimper et al., 2022). We introduce piecewise normalizing flows which divide the target distribution into clusters, with topologies that better match the standard normal base distribution, and train a series of flows to model complex multi-modal targets. We demonstrate the performance of the piecewise flows using some standard benchmarks and compare the accuracy of the flows to the approach taken in Stimper et al. (2022) for modelling multi-modal distributions. We find that our approach consistently outperforms the approach in Stimper et al. (2022) with a higher emulation accuracy on the standard benchmarks.

1. Introduction

Normalizing flows (NF) are an effective tool for emulating probability distributions given a set of target samples. They

¹Kavli Institute for Cosmology, University of Cambridge, Madingley Road, Cambridge, CB3 0HA ²Cavendish Astrophysics, University of Cambridge, Cavendish Laboratory, JJ Thomson Avenue, Cambridge, CB3 0HE. Correspondence to: Harry Thomas Jones Bevins <htjb2@cam.ac.uk>, Will Handley <wh260@cam.ac.uk>, Thomas Gessey-Jones <tg400@cam.ac.uk>.

Proceedings of the 41st International Conference on Machine Learning, Vienna, Austria. PMLR 235, 2024. Copyright 2024 by the author(s).

are bijective and differentiable transformations between a base distribution, often a standard normal distribution, and the target distribution (Papamakarios et al., 2019). They have been applied successfully in a number of fields such as the approximation of Boltzmann distributions (Wirnsberger et al., 2020), cosmology (Alsing & Handley, 2021; Bevins et al., 2022; Friedman & Hassan, 2022), image generation (Ho et al., 2019; Grcić et al., 2021), audio synthesis (van den Oord et al., 2018), density estimation (Papamakarios et al., 2017; Huang et al., 2018) and variational inference (Rezende & Mohamed, 2015) among others.

When the target distribution is multi-modal, NFs can take a long time to train well, and often feature ‘bridges’ between the different modes that are not present in the training data (see Figure 1). These bridges arise due to differences between the topology of the base distribution and the often complex target distribution (Cornish et al., 2019) and is a result of the homeomorphic nature of the NFs (Runde, 2007).

One approach to deal with multi-modal distributions is to modify the topology of the base distribution. This was demonstrated in (Stimper et al., 2022), in which the authors developed a base distribution derived using learned rejection sampling. There are a number of other approaches to solve the mismatch between base and target distribution topologies such as; continuously indexing flows (Cornish et al., 2019), augmenting the space the model fits in (Huang et al., 2018) and adding stochastic layers (Wu et al., 2020) among others.

A few works have attempted to use Gaussian mixture models for the base distribution (e.g. Papamakarios et al., 2017; Izmailov et al., 2020) and have extended various NF structures to perform classification while training. For example, Izmailov et al. (2020) showed that a high degree of accuracy can be accomplished if data is classified in modes in the latent space based on a handful of labelled samples. Ardizzone et al. (2020) uses the information bottleneck to perform classification via a Gaussian mixture model. Similar ideas were explored in Hagemann & Neumayer (2021). Recently, it was shown that the boundaries between different modes could be effectively learnt during training using Voronoi clustering (Chen et al., 2022).

Our main contribution is to classify samples from our

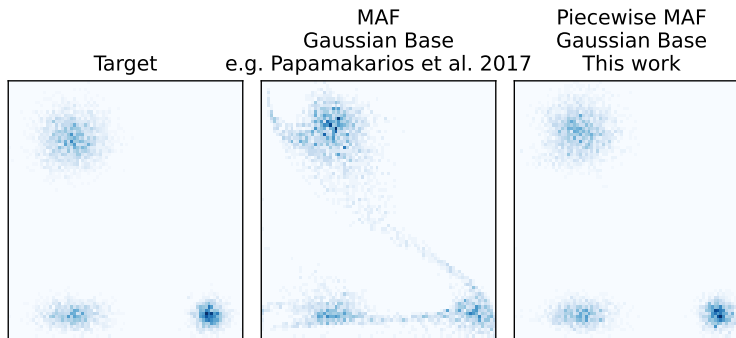


Figure 1. A simple demonstration of the piecewise normalizing flow (NF) described in this paper and a single NF trained on the same multimodal target distribution. We use early stopping to train the different normalizing flows. For the single NF we see bridging between the different clusters that is not present in the piecewise approach. The architecture of the MAF and piecewise MAF components are chosen such that the two have approximately the same number of hyperparameters.

target distribution using a clustering algorithm *before* training and train normalizing flows on the resultant clusters in a piecewise approach where each piece constitutes a NF with a Gaussian base distribution. This improves the accuracy of the flow and reduces the computational resources required for accurate training for two reasons. Firstly, it is parallelizable and each piece can be trained simultaneously, and secondly if sufficient clusters are used, the topology of each piece of the target distributions is closer to that of the Gaussian base distribution. We compare the accuracy of our results against the approach put forward in (Stimper et al., 2022) using a series of benchmark multi-modal distributions.

2. Normalizing Flows

If we have a target distribution X and a base distribution $Z \sim \mathcal{N}(\mu = 0, \sigma = 1)$ then via a change of variables we can write

$$p_X(x) = p_Z(z) \left| \det \left(\frac{\partial z}{\partial x} \right) \right|, \quad (1)$$

where the base distribution is chosen to be Gaussian so that it is easy to sample and evaluate. If there is a bijective transformation between the two f then z is given by $f_\theta^{-1}(x)$ and the change of variable formula becomes

$$p_X(x) = p_Z(f_\theta^{-1}(x)) \left| \det \left(\frac{\partial f_\theta^{-1}(x)}{\partial x} \right) \right|, \quad (2)$$

where θ are the parameters describing the transformation from the base to target distribution. Here, the magnitude of the determinant of the Jacobian represents the volume contraction from p_Z to p_X . The transformation f corresponds to the invertible normalizing flow between p_X and p_Z and θ to the hyperparameters of the flow. In our work we use Masked Autoregressive Flows (MAFs, Papamakarios

et al., 2017) which are based on the Masked Autoencoder for Distribution Estimation (MADEs, Germain et al., 2015).

For a MAF, the multidimensional target distribution is decomposed into a series of one dimensional conditional distributions

$$p_X(x) = \prod_i p(x_i | x_1, x_2, \dots, x_{i-1}), \quad (3)$$

where the index i represents the dimension. Each conditional probability is modelled as a Gaussian distribution with some standard deviation, σ_i , and mean, μ_i , which can be written as

$$P(x_i | x_1, x_2, \dots, x_{i-1}) = \mathcal{N}(\mu_i(x_1, x_2, \dots, x_{i-1}), \sigma_i(x_1, x_2, \dots, x_{i-1})). \quad (4)$$

σ_i and μ_i are functions of θ and are output from the network. The optimum values of the network weights and biases are arrived at by training the network to minimize the Kullback-Leibler (KL) divergence between the target distribution and the reconstructed distribution

$$\mathcal{D}(p_X(x) || p_\theta(x)) = -\mathbb{E}_{p_X(x)}[\log p_\theta(x)] + \mathbb{E}_{p_X(x)}[\log p_X(x)]. \quad (5)$$

The second term in the KL divergence is independent of the network and so for a minimization problem we can ignore this and since

$$-\mathbb{E}_{p_X(x)}[\log p_\theta(x)] = -\frac{1}{N} \sum_{j=0}^N \log p_\theta(x_j), \quad (6)$$

where j corresponds to a sample in the set of N samples, our minimization problem becomes

$$\operatorname{argmin}_\theta - \sum_{j=0}^N \log p_\theta(x_j). \quad (7)$$

In practice the flows are trained to transform samples from the target distribution into samples from the base distribution and the loss is evaluated by a change of variables

$$\operatorname{argmin}_{\theta} - \sum_{j=0}^N \left[\log p_Z(z'_j) + \log \left| \frac{\partial z'_j}{\partial x_j} \right| \right], \quad (8)$$

where z' is a function of θ (Alsing et al., 2019; Stimper et al., 2022). See Fig. 1 of Bevins et al. (2023) for an illustration of the MADE network. Typically, many MADE networks are chained together to improve the expressivity of the MAF (Papamakarios et al., 2017).

3. Clustering and Normalizing Flows

We propose a piecewise approach to learning complex multimodal distributions, in which we decompose the target distribution into clusters before training and train individual MAFs on each cluster. For k clusters of samples x_k we therefore have a set

$$x = \{x_1, x_2, \dots, x_k\} \text{ and } p_{\theta} = \{p_{\theta_1}, p_{\theta_2}, \dots, p_{\theta_k}\}. \quad (9)$$

Typically, if our samples for our target distribution have been drawn with some sample weights, w_j , (i.e. using an MCMC (e.g. Foreman-Mackey et al., 2013) or Nested Sampling (Skilling, 2006; Handley et al., 2015) algorithm) then each set of samples in each cluster has associated weights

$$w = \{w_1, w_2, \dots, w_k\}. \quad (10)$$

and our total loss over N_{clusters} is given by

$$\operatorname{argmin}_{\theta} - \left[\sum_{j=0}^{N_0} w_{0,j} \log p_{\theta_1}(x_{0,j}) + \sum_{j=0}^{N_1} w_{1,j} \log p_{\theta_2}(x_{1,j}) + \dots + \sum_{j=0}^{N_k} w_{k,j} \log p_{\theta_k}(x_{k,j}) \right], \quad (11)$$

which can be written as

$$\operatorname{argmin}_{\theta} - \sum_{k=0}^{N_{\text{cluster}}} \sum_{j=0}^{N_k} w_{k,j} \log p_{\theta_k}(x_{k,j}). \quad (12)$$

Hence, the loss function for the entire network is just the linear sum of the losses for individual cluster MAFs. We thus train each cluster’s MAF separately, using an ADAM optimizer (Kingma & Ba, 2014). Since each cluster constitutes a simpler target distribution than the whole, we find that we need fewer computing resources when training a piecewise NF in comparison to training a single NF on the same problem (see Section 4 and Table 2). One can train each piece of the PNF in parallel, leading to further (wall time) computational gains.

To determine the number of clusters needed to best describe the target distribution, we use an average silhouette score, where the silhouette score for an individual sample is a measure of how similar a sample is with the samples in its cluster compared to samples outside its cluster (Rousseeuw, 1987). The score ranges between -1 and 1 and peaks when the clusters are clearly separated and well-defined, as in Figure 2.

Our approach is independent of the choice of clustering algorithm (see Section 4.2), however in this paper we use the k -means algorithm (Steinhaus, 1957; MacQueen, 1967).

We can draw samples from each cluster in a trained piecewise normalizing flow with a weight given by the total weight in the target cluster, $\mathcal{W}_k = \sum_{j=0}^{N_k} w_{j,k}$. This process is shown in Figure 3 along with the general flow of classification and training.

The probability of our piecewise MAF for a sample, x , is given by

$$\log p_{\theta}(x) = \log \left(\sum_k \mathcal{W}_k \exp \left(\log p_{\theta_k}(x) \right) \right) - \log \left(\sum_k \mathcal{W}_k \right), \quad (13)$$

or equivalently

$$\log p_{\theta}(x) = \log \left(\sum_k \left[\exp \left(\log(\mathcal{W}_k) + \log(p_{\theta,k}) \right) \right] \right) - \log \left(\sum_k \mathcal{W}_k \right), \quad (14)$$

and if we normalize \mathcal{W}_k such that the sum is equal to one we arrive at

$$\log p_{\theta}(x) = \log \left(\sum_k \left[\exp \left(\log(\mathcal{W}_k) + \log(p_{\theta,k}) \right) \right] \right). \quad (15)$$

From this we can calculate the KL divergence and an associated Monte Carlo error

$$D_{KL} = \left\langle \log \frac{p_{\theta}(x)}{p_X(x)} \right\rangle_{p_{\theta}(x)} \pm \frac{1}{\sqrt{N}} \sigma \left(\log \frac{p_{\theta}(x)}{p_X(x)} \right)_{p_{\theta}(x)}, \quad (16)$$

where $p_X(x)$ is the analytic target distribution, N samples $x \sim p_{\theta}(x)$ and $\sigma(f)_g$ is the standard deviation of f with respect to g .

4. Benchmarking

4.1. Toy Models

We test our piecewise normalizing flow on a series of multimodal problems that are explored in (Stimper et al., 2022).

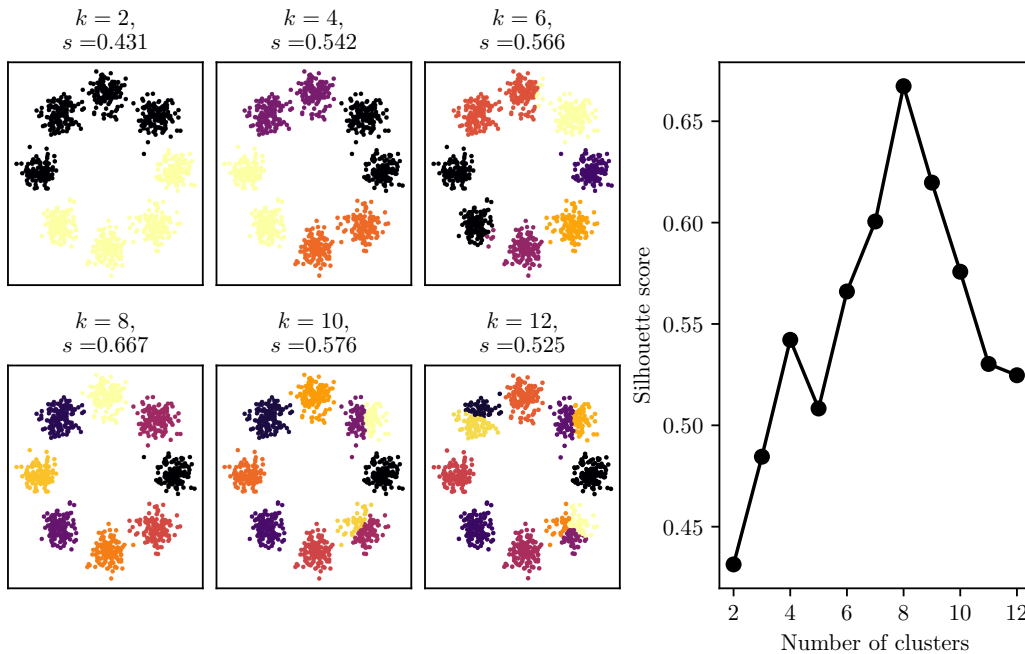


Figure 2. The figure shows how the silhouette score, s , can be used to determine the number of clusters needed to describe the data. In the example s peaks for eight clusters corresponding to one for each Gaussian in the circle.

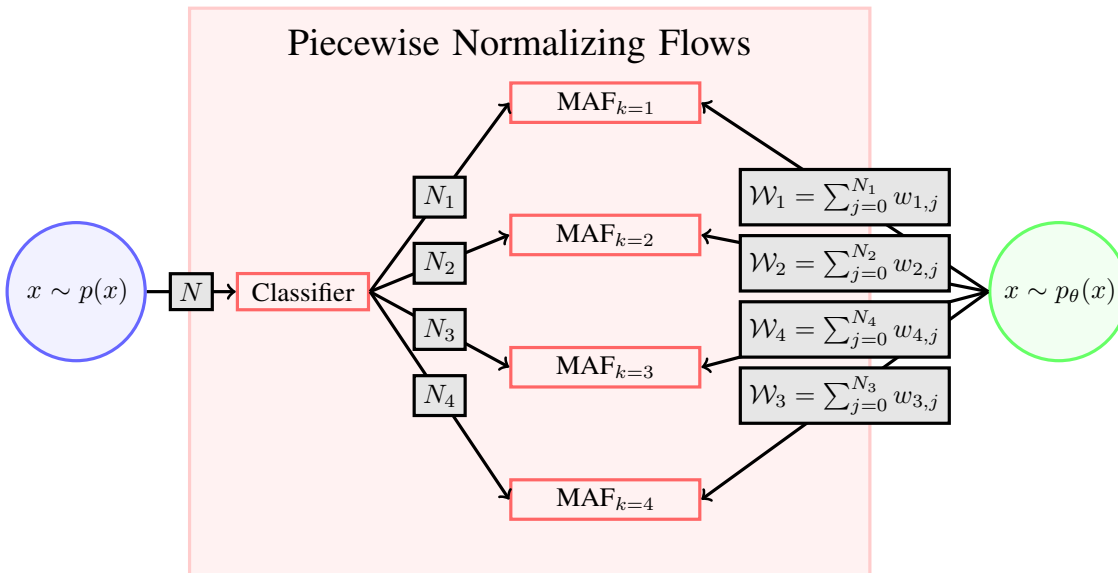


Figure 3. The figure shows the training and sampling process for our piecewise NFs. From left to right, we start with a set of samples x drawn from $p_X(x)$ and classify the samples into clusters (e.g. using k -means), determining the number of clusters to use based on the silhouette score. We then train a Masked Autoregressive Flow on each cluster k using a standard normal distribution as our base. When drawing samples from $p_\theta(x)$ we select which MAF to draw from using weights defined according to the total cluster weight.

Distribution	KL divergence		
	MAF Gaussian Base e.g. (Papamakarios et al., 2017)	RealNVP Resampled Base (Stimper et al., 2022)	Piecewise MAF Gaussian Base This work
Two Moons	-0.054 ± 0.009	0.028 ± 0.055	0.004 ± 0.022
Circle of Gaussians	-0.046 ± 0.050	0.231 ± 0.138	0.001 ± 0.005
Two Rings	0.015 ± 0.078	0.080 ± 0.106	0.031 ± 0.032

Table 1. The table shows the KL divergence between the target samples for a series of multi-modal distributions and the equivalent representations with a single MAF, a RealNVP with a resampled base distribution (e.g. Stimper et al., 2022) and a piecewise MAF. We train each type of flow on the target distributions ten times. The reported KL divergences are the mean over the ten training runs. The error for each training run is calculated as in Equation (16) and the errors are added in quadrature across training runs to get the error on the mean KL. The distributions and an example set of samples drawn from each of the flows is shown in Figure 4. We have used early stopping for training and each flow has approximately the same number of hyperparameters. We find that our piecewise approach is competitive to the approach detailed in (Stimper et al., 2022) for modelling multi-modal probability distributions and, since the KL divergence have a smaller error, more consistent over repeated training runs. Negative KL divergences are a result of the Monte Carlo nature of the calculation.

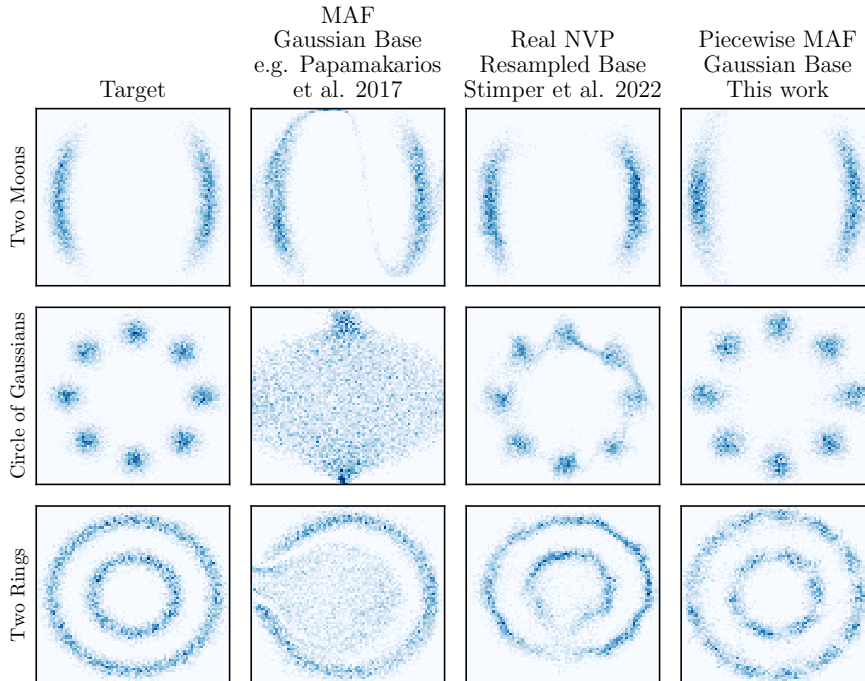


Figure 4. The graph shows a series of multi-modal target distributions as 2D histograms of samples in the first column and three representations of this distribution produced with three different types of normalizing flow. We use early stopping, as described in the main text, to train all the normalizing flows. The second column shows a simple Masked Autoregressive Flow with a Gaussian base distribution based on the work in (Papamakarios et al., 2017) and the later two columns show two approaches to improve the accuracy of the model. The first is from (Stimper et al., 2022) and uses a RealNVP flow to model the distributions while resampling the base distribution to better match the topology of the target distribution. In the last column, we show the results from our PNFs, where we have effectively modified the topology of the target distribution to better match the Gaussian base distribution by performing clustering.

For each, we model the distribution using a single MAF with a Gaussian base distribution, a RealNVP with a resampled base distribution as in [Stimper et al. \(2022\)](#) and our piecewise MAF approach. While there are a number of different methods for accurately learning multimodal distributions, the vast majority are not bijective unlike the approach taken in [Stimper et al. \(2022\)](#) and so we compare our results with that method. We calculate the Kullback-Leibler divergence between the original target distribution and the trained flows to assess the performance of the different methods.

We show the target distributions and samples drawn from each type of flow, a MAF, a piecewise MAF and a RealNVP with a resampled base distribution, in [Figure 4](#) and report the corresponding KL divergences in [Table 1](#). We train each flow ten times and calculate an average KL divergence for each flow and distribution. We add the associated Monte Carlo errors in quadrature to get an error on the mean KL divergence. We find that our piecewise approach outperforms the resampled base distribution approach of [Stimper et al. \(2022\)](#) for all of our multi-modal benchmarks. We use the code available at <https://github.com/VincentStimper/resampled-base-flows> to fit the RealNVP flows and the code MARGARINE ([Bevins et al., 2023; 2022](#)) available at <https://github.com/htjb/margarine> to fit the MAFs and PNFs. We chose the architecture of the MAF, PNF and RealNVP such that they have approximately the same number of hyperparameters.

We use early stopping to train all the flows in the paper, including the RealNVP resampled base models from [Stimper et al. \(2022\)](#). For the single MAF and RealNVP, we use 20% of the samples from our target distribution as test samples. We early stop when the minimum test loss has not improved for 2% of the maximum iterations requested, 10,000 for all examples in this paper, and roll back to the optimum model. For the PNF, we split each cluster into training and test samples and perform early stopping on each cluster according to the same criterion, meaning that each cluster is trained for a different number of epochs. All the experiments in this paper were run on an Apple MacBook Pro with an M2 chip and 8GB memory.

In [Table 2](#), we report the cost of training, the number of epochs needed and the time taken on average to train a MAF, RealNVP and a PNF on the benchmark distributions five times. We define the cost of training the MAF and RealNVP as the product of the number of epochs, E , the length of the training and test data combined N and the number of hyperparameters in the network h

$$\mathcal{C} = ENh, \tag{17}$$

the idea being that at each epoch we do h calculations N times (since we evaluate both the test and training loss).

For the PNF each piece of the distribution is trained on a fraction of the data, for a different number of epochs and each MAF in the PNF has $h_k < h$ such that $\sum_k h_k \approx h$. The cost of such a ‘divide and conquer’ approach is given by

$$\mathcal{C} = \sum_k E_k N_k h_k. \tag{18}$$

We report the cost and associated errors for the RealNVP and PNF normalized to the value for the MAF for ease of comparison. We find that the RealNVP requires the fewest number of epochs and has the smallest wall clock time. However, the reported wall clock time for the PNF corresponds to training each piece in series and can be made more competitive with the RealNVP through parallelisation. This is represented in the significantly lower costs for PNF training.

4.2. Choosing a clustering algorithm

Next, we illustrate how the choice of clustering algorithm can impact the accuracy of the PNF. We repeat the analysis from the previous section on the two rings distribution, using five different clustering algorithms to perform the initial division of the target samples.

So far, we have employed the k -means clustering algorithm to identify clusters in the target distribution. Here we test Mini-batch k -means ([Sculley, 2010](#)), the Mean Shift algorithm ([Cheng, 1995](#)), Spectral Clustering ([Shi & Malik, 2000](#)), Agglomerative Clustering ([Nielsen, 2016](#)) and the Birch algorithm ([Zhang et al., 1996](#)). All of these algorithms are readily accessible through the SKLEARN PYTHON package which we used with the default settings, and we refer the reader to the review by [Saxena et al. \(2017\)](#) for more details.

For each clustering algorithm, we run training ten times and calculate a KL divergence between the target distribution and the PNF according to [Equation \(16\)](#). The mean KL divergence values over training runs and an associated error are reported in [Table 3](#). We can clearly see that the k -means algorithm outperforms the others but that Mean Shift and Birch clustering competitive with each other, k -means and the RealNVP resampled base approach.

This work is not intended to be an exhaustive search of available clustering algorithms, however, it illustrates that PNFs can be built with different clustering algorithms. We recommend k -means, Mean Shift and Birch clustering based on the results presented here but stress that the choice of clustering algorithm may be data dependent.

4.3. Physical Examples

It is common to compare proposed normalizing flow architectures on data sets from the UCI machine learning

Cost			
Distribution	MAF	RealNVP	PNF
Two Moons	1.000 ± 0.191	0.241 ± 0.003	0.225 ± 0.037
Circle of Gaussians	1.000 ± 0.206	0.794 ± 0.092	0.226 ± 0.005
Two Rings	1.000 ± 0.265	0.800 ± 0.098	0.236 ± 0.007

Epochs			
Distribution	MAF	RealNVP	PNF
Two Moons	3131 ± 598	655 ± 9	2118 ± 351
Circle of Gaussians	1765 ± 364	1217 ± 141	19130 ± 412
Two Rings	1896 ± 503	1317 ± 162	42444 ± 1720

Wall Time [s]			
Distribution	MAF	RealNVP	PNF
Two Moons	72.80 ± 12.72	4.05 ± 0.05	22.72 ± 3.31
Circle of Gaussians	42.13 ± 8.49	7.62 ± 0.86	26.47 ± 1.15
Two Rings	46.02 ± 12.14	8.33 ± 1.04	44.55 ± 1.82

Table 2. The table summarises the cost of training, the total number of epochs and the wall time for a MAF, a RealNVP and a PNF on the three toy example distributions explored in this paper. The values are averages over five training runs with an associated Monte Carlo error. Here the cost, as defined in the text, and the associated error are normalized to the MAF value to aid the comparison. Of the three tested algorithms the RealNVP requires the fewest epochs to train and has the shortest wall time. However, the cost to train the PNF is significantly lower than the RealNVP and MAF because the data are distributed over several smaller MAFs with fewer hyperparameters. It should be noted that the total wall clock time for the PNF corresponds to training the pieces in series and through parallelisation the PNF wall clock time can be made competitive with the RealNVP. This is represented in the cost.

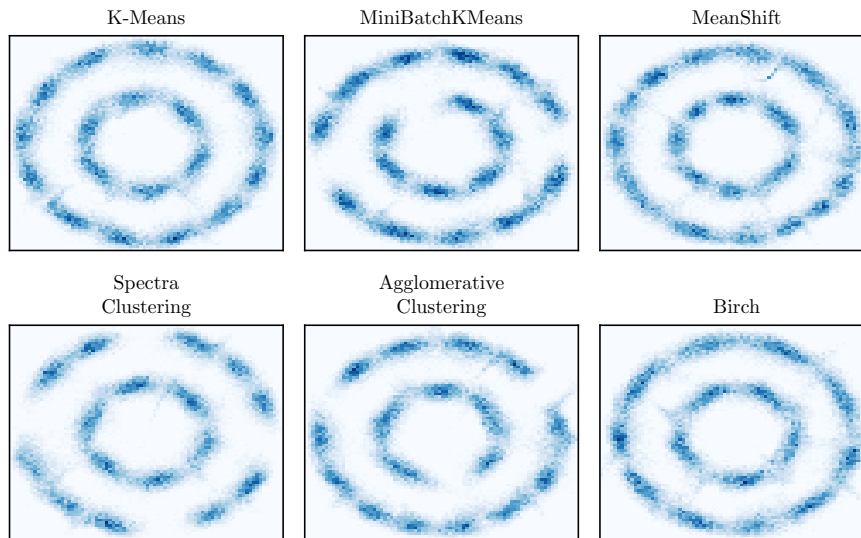


Figure 5. The figure shows samples drawn from various different PNFs built using different clustering algorithms, along with samples from the true distribution and samples from a single masked autoregressive flow. The figure illustrates that the PNF can be effectively built from using different clustering algorithms and, along with Table 3, that some clustering algorithms perform better than others. We choose network architectures for our PNFs and MAF such that they all have approximately the same number of hyperparameters.

Flow Type	D_{KL}
MAF	0.015 ± 0.078
RealNVP Resampled Base	0.080 ± 0.106
PNF k -means	0.031 ± 0.032
PNF Mini-batch k -means	0.847 ± 0.038
PNF Mean Shift	0.040 ± 0.007
PNF Spectral Clustering	0.814 ± 0.035
PNF Agglomerative Clustering	0.419 ± 0.028
PNF Birch	0.036 ± 0.007

Table 3. The table shows the KL divergence between the target distribution, the two rings toy example, and a series of different PNFs built with different clustering algorithms, a single MAF and the RealNVP with a resampled base distribution. The values for the MAF, RealNVP and k -means PNF are drawn from Table 1. We find that k -means is the best of the tested clustering algorithms, but that Mean Shift and Birch Clustering are competitive with the RealNVP.

Flow Type	POWER (6)	GAS (8)
MAF	-0.05 ± 0.08	5.10 ± 0.09
PNF	-0.09 ± 0.07	4.32 ± 0.68

Flow Type	HEPMASS (21)	MINIBOONE (43)
MAF	-20.11 ± 0.02	-11.63 ± 0.44
PNF	-20.71 ± 0.02	-12.40 ± 0.45

Table 4. We compare the accuracy of the PNF proposed here with a single MAF on four data sets from the UCI machine learning repository (Kelly et al., 2023). The table shows the average log-likelihood evaluated over a test data set for the POWER, GAS, HEPMASS and MINIBOONE UCI data sets. We show the number of dimensions for each data set in brackets. Generally speaking, the MAF performs better than the PNF however Papamakarios et al. (2017) previously found that generally the data sets could be better modelled with a MAF with a standard normal base distribution over a Gaussian mixture base distribution suggesting that the data sets are not significantly multi-modal. Again we use early stopping during training and note that the PNF and MAF have approximately the same number of hyperparameters. Errors are two sigma as in Papamakarios et al. (2017).

repository (Kelly et al., 2023). Accuracy of emulation is assessed by evaluating the average log-probability over the flow for a set of unseen test samples. A higher average log-probability indicates a more accurate network, which can be seen from the discussion of the loss function in Section 2. We report the results of training on four UCI datasets (POWER, GAS, HEPMASS and MINIBOONE) in Table 4 along with an associated Monte Carlo error bar.

The POWER and GAS data sets are much larger than HEPMASS and MINIBOONE and consequently computationally expensive to train on. We therefore took representative subsets of these two data sets for training and testing.

Generally, speaking the MAF performs better on these physical data sets when compared to the PNF although the PNF is competitive for the POWER and GAS data sets. We note that there is no indication in the literature that these data sets are multi-modal. For example, Papamakarios et al. (2017) find that generally MAFs with standard normal base distributions perform better on these targets compared to MAFs with Gaussian Mixture model base distributions. We therefore do not necessarily expect the PNFs to perform better than the MAFs, as was shown for the toy multi-modal cases. Indeed, for all the data sets we see a preference via the silhouette score for the minimum tested number of clusters, 2. It is reassuring, however, that the PNF does not perform drastically worse than the MAF on these examples.

5. Limitations

Normalizing flows are useful because they are bijective and differentiable, however these properties are sometimes lost when trying to tackle multi-modal distributions. Our piecewise approach is differentiable, provided that the optimization algorithm used to classify the samples from the target distribution into clusters is also differentiable and k , the number of clusters, is fixed during training.

Our piecewise approach is bijective if we know the cluster that our sample has been drawn from. In other words, there is a one to one mapping between a set of real numbers drawn from an N dimensional base distribution to a set of real numbers on the N dimensional target distribution plus a cluster number, $n \in \mathbb{N}$

$$\mathbb{R}_{\mathcal{N}(\mu=0, \sigma=1)}^N \iff \mathbb{R}_{p_\theta(x)}^N \times \mathbb{N}. \quad (19)$$

6. Conclusions

In this work, we demonstrate a new method for accurately learning multi-modal probability distributions with normalizing flows through the aid of an initial classification of the target distribution into clusters.

Normalizing flows generally struggle with multi-modal distributions because there is a significant difference in the topology of the base distribution and the target distribution to be learnt. By dividing our target distribution up into clusters, we are essentially, for each piece, making the topology of the target distribution more like the topology of our base distribution, leading to an improved expressivity. Stimper et al. (2022) by contrast, resampled the base distribution so that it and the target distribution shared a more similar topology. We find that both approaches perform well on our benchmark tests, but that our piecewise approach is better able to capture the distributions when training with early stopping. The piecewise nature of our approach allows the MAFs to be trained in parallel.

Through the combination of clustering and normalizing flows, we are able to produce accurate representations of complex multi-modal probability distributions.

7. Acknowledgements

HTJB acknowledges support from the Kavli Institute for Cosmology, Cambridge, the Kavli Foundation and of St Edmunds College, Cambridge. WJH thanks the Royal Society for their support through a University Research Fellowship. TGJ would like to thank the Science and Technology Facilities Council (UK) for their continued support through grant number ST/V506606/1.

This work used the DiRAC Data Intensive service (CSD3) at the University of Cambridge, managed by the University of Cambridge University Information Services on behalf of the STFC DiRAC HPC Facility (www.dirac.ac.uk). The DiRAC component of CSD3 at Cambridge was funded by BEIS, UKRI and STFC capital funding and STFC operations grants. DiRAC is part of the UKRI Digital Research Infrastructure.

8. Impact Statement

Bias in machine learning is currently an active area of concern and research (e.g. [Jiang & Nachum, 2020](#); [Mehrabi et al., 2021](#)). While we have focused on normalizing flows for probability density estimation in this work, we believe that the general approach has wider applications. One can imagine dividing a training data set into different classes and training a series of generative models to produce new data. One could then draw samples based on user defined weights rather than data defined weights, as is done here. As such, one can begin to overcome some selection biases when training machine learning models. Of course the ‘user determined’ nature of the weights could be used to introduce more bias into the modelling, therefore the method through which they are derived would have to be explicit and ethically sound.

References

Alsing, J. and Handley, W. Nested sampling with any prior you like. *Monthly Notices of the Royal Astronomical Society*, 505(1):L95–L99, July 2021. doi: 10.1093/mnras/ slab057.

Alsing, J., Charnock, T., Feeney, S., and Wandelt, B. Fast likelihood-free cosmology with neural density estimators and active learning. *Monthly Notices of the Royal Astronomical Society*, 488(3):4440–4458, September 2019. doi: 10.1093/mnras/stz1960.

Ardizzone, L., Mackowiak, R., Rother, C., and Köthe, U.

Training normalizing flows with the information bottleneck for competitive generative classification. *Advances in Neural Information Processing Systems*, 33: 7828–7840, 2020.

Bevins, H., Handley, W., Lemos, P., Sims, P., de Lera Acedo, E., and Fialkov, A. Marginal Bayesian Statistics Using Masked Autoregressive Flows and Kernel Density Estimators with Examples in Cosmology. *arXiv e-prints*, art. arXiv:2207.11457, July 2022.

Bevins, H. T. J., Handley, W. J., Lemos, P., Sims, P. H., de Lera Acedo, E., Fialkov, A., and Alsing, J. Marginal post-processing of Bayesian inference products with normalizing flows and kernel density estimators. *Monthly Notices of the Royal Astronomical Society*, 526(3):4613–4626, December 2023. doi: 10.1093/mnras/stad2997.

Chen, R. T., Amos, B., and Nickel, M. Semi-discrete normalizing flows through differentiable tessellation. *Advances in Neural Information Processing Systems*, 35: 14878–14889, 2022.

Cheng, Y. Mean shift, mode seeking, and clustering. *IEEE Transactions on Pattern Analysis and Machine Intelligence*, 17(8):790–799, 1995. doi: 10.1109/34.400568.

Cornish, R., Caterini, A. L., Deligiannidis, G., and Doucet, A. Relaxing bijectivity constraints with continuously indexed normalising flows. In *International Conference on Machine Learning*, 2019.

Foreman-Mackey, D., Hogg, D. W., Lang, D., and Goodman, J. emcee: The MCMC Hammer. *Publications of the Astronomical Society of the Pacific*, 125(925):306, March 2013. doi: 10.1086/670067.

Friedman, R. and Hassan, S. HIGlow: Conditional Normalizing Flows for High-Fidelity HI Map Modeling. *arXiv e-prints*, art. arXiv:2211.12724, November 2022. doi: 10.48550/arXiv.2211.12724.

Germain, M., Gregor, K., Murray, I., and Larochelle, H. MADE: Masked Autoencoder for Distribution Estimation. *arXiv e-prints*, art. arXiv:1502.03509, February 2015. doi: 10.48550/arXiv.1502.03509.

Grcić, M., Grubišić, I., and Šegvić, S. Densely connected normalizing flows. In Ranzato, M., Beygelzimer, A., Dauphin, Y., Liang, P., and Vaughan, J. W. (eds.), *Advances in Neural Information Processing Systems*, volume 34, pp. 23968–23982. Curran Associates, Inc., 2021. URL https://proceedings.neurips.cc/paper_files/paper/2021/file/c950cde9b3f83f41721788e3315a14a3-Paper.pdf.

- Hagemann, P. and Neumayer, S. Stabilizing invertible neural networks using mixture models. *Inverse Problems*, 37(8): 085002, 2021.
- Handley, W. J., Hobson, M. P., and Lasenby, A. N. POLYCHORD: next-generation nested sampling. *Monthly Notices of the Royal Astronomical Society*, 453(4):4384–4398, November 2015. doi: 10.1093/mnras/stv1911.
- Ho, J., Chen, X., Srinivas, A., Duan, Y., and Abbeel, P. Flow++: Improving flow-based generative models with variational dequantization and architecture design. In Chaudhuri, K. and Salakhutdinov, R. (eds.), *Proceedings of the 36th International Conference on Machine Learning*, volume 97 of *Proceedings of Machine Learning Research*, pp. 2722–2730. PMLR, 09–15 Jun 2019. URL <https://proceedings.mlr.press/v97/ho19a.html>.
- Huang, C.-W., Krueger, D., Lacoste, A., and Courville, A. Neural autoregressive flows. In Dy, J. and Krause, A. (eds.), *Proceedings of the 35th International Conference on Machine Learning*, volume 80 of *Proceedings of Machine Learning Research*, pp. 2078–2087. PMLR, 10–15 Jul 2018. URL <https://proceedings.mlr.press/v80/huangl8d.html>.
- Izmailov, P., Kirichenko, P., Finzi, M., and Wilson, A. G. Semi-supervised learning with normalizing flows. In *International Conference on Machine Learning*, pp. 4615–4630. PMLR, 2020.
- Jiang, H. and Nachum, O. Identifying and correcting label bias in machine learning. In *International Conference on Artificial Intelligence and Statistics*, pp. 702–712. PMLR, 2020.
- Kelly, M., Longjohn, R., and Nottingham, K. The uci machine learning repository, 2023. URL <https://archive.ics.uci.edu>.
- Kingma, D. P. and Ba, J. Adam: A method for stochastic optimization. *CoRR*, abs/1412.6980, 2014.
- MacQueen, J. B. Some methods for classification and analysis of multivariate observations. In Cam, L. M. L. and Neyman, J. (eds.), *Proc. of the fifth Berkeley Symposium on Mathematical Statistics and Probability*, volume 1, pp. 281–297. University of California Press, 1967.
- Mehrabi, N., Morstatter, F., Saxena, N., Lerman, K., and Galstyan, A. A survey on bias and fairness in machine learning. *ACM Comput. Surv.*, 54(6), jul 2021. ISSN 0360-0300. doi: 10.1145/3457607. URL <https://doi.org/10.1145/3457607>.
- Nielsen, F. *Hierarchical Clustering*, pp. 195–211. 02 2016. ISBN 978-3-319-21902-8. doi: 10.1007/978-3-319-21903-5_8.
- Papamakarios, G., Pavlakou, T., and Murray, I. Masked autoregressive flow for density estimation. In Guyon, I., Luxburg, U. V., Bengio, S., Wallach, H., Fergus, R., Vishwanathan, S., and Garnett, R. (eds.), *Advances in Neural Information Processing Systems*, volume 30. Curran Associates, Inc., 2017. URL https://proceedings.neurips.cc/paper_files/paper/2017/file/6c1da886822c67822bcf3679d04369fa-Paper.pdf.
- Papamakarios, G., Nalisnick, E. T., Rezende, D. J., Mohamed, S., and Lakshminarayanan, B. Normalizing flows for probabilistic modeling and inference. *J. Mach. Learn. Res.*, 22:57:1–57:64, 2019.
- Rezende, D. and Mohamed, S. Variational inference with normalizing flows. In Bach, F. and Blei, D. (eds.), *Proceedings of the 32nd International Conference on Machine Learning*, volume 37 of *Proceedings of Machine Learning Research*, pp. 1530–1538, Lille, France, 07–09 Jul 2015. PMLR. URL <https://proceedings.mlr.press/v37/rezende15.html>.
- Rousseeuw, P. J. Silhouettes: A graphical aid to the interpretation and validation of cluster analysis. *Journal of Computational and Applied Mathematics*, 20:53–65, 1987. ISSN 0377-0427. doi: [https://doi.org/10.1016/0377-0427\(87\)90125-7](https://doi.org/10.1016/0377-0427(87)90125-7). URL <https://www.sciencedirect.com/science/article/pii/0377042787901257>.
- Runde, V. *A Taste of Topology*. Springer, 2007.
- Saxena, A., Prasad, M., Gupta, A., Bharill, N., Patel, O. P., Tiwari, A., Er, M. J., Ding, W., and Lin, C.-T. A review of clustering techniques and developments. *Neurocomputing*, 267:664–681, 2017. ISSN 0925-2312. doi: <https://doi.org/10.1016/j.neucom.2017.06.053>. URL <https://www.sciencedirect.com/science/article/pii/S0925231217311815>.
- Sculley, D. Web-scale k-means clustering. WWW ’10, pp. 1177–1178, New York, NY, USA, 2010. Association for Computing Machinery. ISBN 9781605587998. doi: 10.1145/1772690.1772862. URL <https://doi.org/10.1145/1772690.1772862>.
- Shi, J. and Malik, J. Normalized cuts and image segmentation. *IEEE Transactions on Pattern Analysis and Machine Intelligence*, 22(8):888–905, 2000. doi: 10.1109/34.868688.
- Skilling, J. Nested sampling for general Bayesian computation. *Bayesian Analysis*, 1(4):833 – 859, 2006. doi: 10.1214/06-BA127. URL <https://doi.org/10.1214/06-BA127>.

- Steinhaus, H. Sur la division des corps matériels en parties. *Bull. Acad. Pol. Sci., Cl. III*, 4:801–804, 1957. ISSN 0001-4095.
- Stimper, V., Schölkopf, B., and Miguel Hernandez-Lobato, J. Resampling base distributions of normalizing flows. *Proceedings of The 25th International Conference on Artificial Intelligence and Statistics*, 151:4915–4936, 28–30 Mar 2022. URL <https://proceedings.mlr.press/v151/stimper22a.html>.
- van den Oord, A., Li, Y., Babuschkin, I., Simonyan, K., Vinyals, O., Kavukcuoglu, K., van den Driessche, G., Lockhart, E., Cobo, L., Stimberg, F., Casagrande, N., Grewe, D., Noury, S., Dieleman, S., Elsen, E., Kalchbrenner, N., Zen, H., Graves, A., King, H., Walters, T., Belov, D., and Hassabis, D. Parallel WaveNet: Fast high-fidelity speech synthesis. In Dy, J. and Krause, A. (eds.), *Proceedings of the 35th International Conference on Machine Learning*, volume 80 of *Proceedings of Machine Learning Research*, pp. 3918–3926. PMLR, 10–15 Jul 2018. URL <https://proceedings.mlr.press/v80/oord18a.html>.
- Wirnsberger, P., Ballard, A. J., Papamakarios, G., Abercrombie, S., Racanière, S., Pritzel, A., Jimenez Rezende, D., and Blundell, C. Targeted free energy estimation via learned mappings. *The Journal of Chemical Physics*, 153(14):144112, 2020. doi: 10.1063/5.0018903. URL <https://doi.org/10.1063/5.0018903>.
- Wu, H., Köhler, J., and Noé, F. Stochastic normalizing flows. *Advances in Neural Information Processing Systems*, 33: 5933–5944, 2020.
- Zhang, T., Ramakrishnan, R., and Livny, M. Birch: An efficient data clustering method for very large databases. *SIGMOD Rec.*, 25(2):103–114, jun 1996. ISSN 0163-5808. doi: 10.1145/235968.233324. URL <https://doi.org/10.1145/235968.233324>.